ELSEVIER

Polymer 41 (2000) 2431–2438

polymer

Solid state ^{13}C nuclear magnetic resonance for polyguanidines

A.R. Lim[a,*], J.H. Kim[b], B.M. Novak[b]

[a]*Department of Physics, Jeonju University, Jeonju 560-759, South Korea*
[b]*Department of Chemistry, North Carolina State University, Raleigh, NC 27695-8204, USA*

Received 18 December 1998; received in revised form 9 April 1999; accepted 21 June 1999

Abstract

The structure and variations in dynamic motions of three polyguanidines possessing different side chains were studied by ^{13}C CP/MAS NMR. From these results, the structures of the polyguanidines were confirmed, and the ^{13}C spin–lattice relaxation times in the rotating frame were measured. The polyguanidine backbone mobilities were measured as a function of size and chemical make up (aliphatic vs. aromatic). The main-chain carbon of polyguanidine (II) with aromatic side chains has a higher activation energy, 23.12 kJ/mol, than the polyguanidine (I) with aliphatic side chains, 19.76 kJ/mol. Also, the activation energy of the main-chain carbons of polyguanidine (II) and (III) with aromatic side chains was found to depend on the size of side chains.

Keywords: Structural analysis; NMR spectroscopy; Spin–lattice relaxation

1. Introduction

We are interested in designing helical polyguanidines that possess tailored helix reversal barriers [1,2]. One goal is to design helices with high inversion barriers so that racemization between these conformations does not occur. Preliminary results obtained from helical-sense-selective polymerizations of di-*n*-hexylcarbodiimide with a chiral catalyst indicates a barrier size that allows racemization to occur slowly at room temperature [3]. Of the synthetic polymers that exhibit some degree of conformational order, the helical subclass (e.g. polyisocyantes and polyguanidines) has been of particular interest. These polymers are best modeled as single macromolecular chains that can possess regions of right- and left-handed screw senses, separated by helix reversals (i.e. conformations that change the signs of the backbone dihedral angles defining the helical sense) (Scheme 1). The helical conformation is chiral with the left- and right-handed senses having an enantiomeric relationship (Scheme 2).

As a precursor to side chains capable of raising this barrier, we have attempted to use ^{13}C CP/MAS to measure backbone mobilities. Ultimately, we would like to correlate these molecular motions to observed chiro-optical properties.

The ^{13}C NMR has proved to be a very powerful technique for studying the local dynamics of polymers. The ^{13}C spin–lattice relaxation time is the important experimental quantity for probing the dynamical processes. Since the ^{13}C nucleus is of low natural abundance, the relaxation is dominated by the dipolar interactions with the directly bonded hydrogens. By studying the relaxation of the nuclei in different environments within the chain, it is possible to obtain a detailed picture of the motions occurring in different parts of the chain. The measured relaxation data can be used to obtain information about the dynamical processes occurring in different parts of the chain [4,5]. Recent studies have shown that more localized motions, i.e. mobility of the backbone, should be considered along with the conformational transitions, in order to understand the differences in the dynamics of the C–H vectors at different sites of the backbone [6,7]. The ^{13}C $T_{1\rho}$ relaxation parameter is particularly informative since it is directly related to those motions of glassy polymer main chains in the low- to mid-kHz frequency range which are vital in determining mechanical properties such as toughness [8]. The main-chain motions of various polycarbonates at room temperature have been determined from ^{13}C spin–lattice relaxation measurements employing high-resolution techniques, including magic-angle spinning [9,10].

Herein, we confirmed the structures of poly(di-*n*-hexyl)-carbodiimide I, poly(di-*m*-tolylcarbodiimide) II, and poly-(di-benzylcarbodiimide) III, using ^{13}C CP/MAS NMR. Also, the ^{13}C spin–lattice relaxation times in the rotating

* Corresponding author. Tel.: +82-652-220-2514; fax: +82-652-220-2362.
E-mail address: aeranlim@hanmail.net (A.R. Lim)

0032-3861/00/$ - see front matter
PII: S0032-3861(99)00431-0

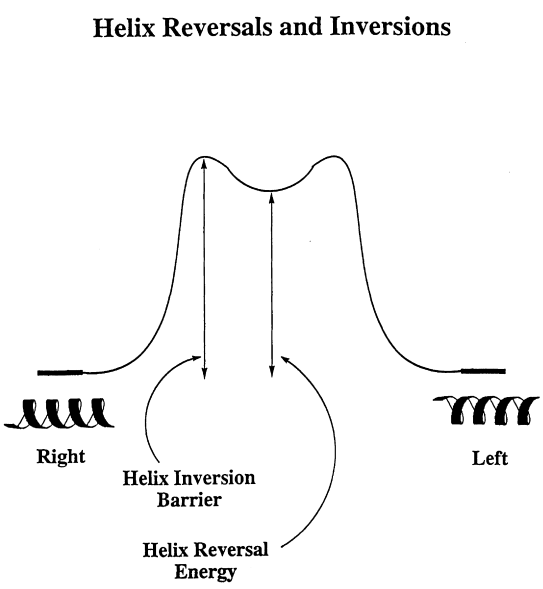

Scheme 1.

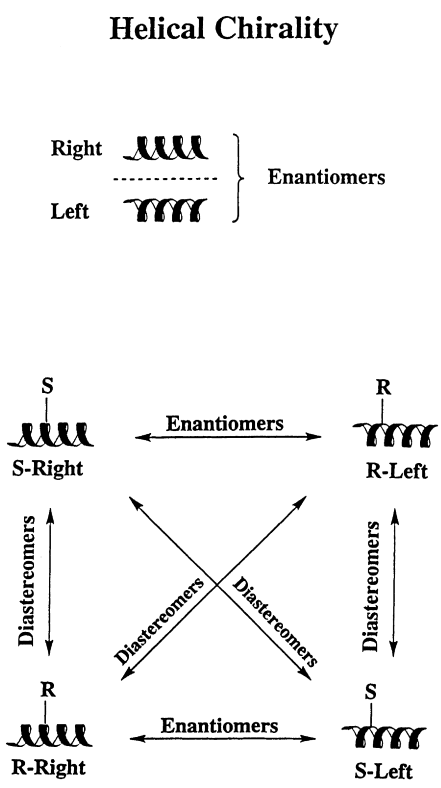

Scheme 2.

frame were measured as a function of temperature. From these results, we discuss the mobility, the correlation time, and the activation energy for each carbon of the polyguanidines as a function of the aliphatic side chains, substituent size and aromatic side chains.

2. Experimental

2.1. Preparation of monomers

All starting materials were obtained from commercial suppliers and used as received. The carbodiimide monomers were prepared with slight modifications to literary [11] procedures. Bischloro-η^5-cyclopentadieny-dimethylamido titanium(IV) was prepared by modifying the procedure of Pattern [12] and Goodwin [13].

Di-m-Tolylcarbodiimide. Here *m*-Tolylisocyanate was prepared (12.9 ml, 0.10 mol) in dry benzene (amount) in a 100 ml round-bottomed flask fitted with a magnetic stirrer. Polystyrene diphenyl arsine oxide catalyst [14] 0.1 g was added and the mixture was allowed to refluxed for 24 h. The catalyst was removed by filtration, and the filtrate was distilled under reduced pressure to yield di-*m*-tolylcarbodiimide. Yield: 9.8 g (88%). ^{1}H NMR(300 MHz, $CDCl_3$): δ (ppm) 2.44 (s, 6H, CH_3), 7.10 (t, 4H, Ar), 7.30 (t, 2H, Ar). IR (neat): 3031(m), 3016(m), 2915(m), 2851(m), 2135(vs), 1597(s), 1581(s), 1481(s), 1432(m), 1245(s) cm^{-1}.

Dibenzylurea. Benzylamine (8.84 ml, 81.1 mmol) was slowly added, in drops, to a solution of 200 ml dry chloroform and 10.0 ml benzylisocyanate (81.1 mmol) equipped with a 250 ml round-bottomed flask. Additional $CHCl_3$ (20 ml) was used to ensure complete transfer of the benzylamine. The resultant solution was stirred for 1 h. The solid dibenzylurea was obtained by rotary evaporation and recrystallized in ethanol. Yield: 18.1 g (92%). ^{1}H NMR (300 MHz, $CDCl_3$): δ (ppm) 4.15 (s, 4H, CH_2), 5.05 (s, 2H, NH), 7.15 (m, 10H, Ar). IR (KBr pellet): 3344(m), 3344(m), 3030(m), 3015(m), 2915(m), 2820(vs), 1622(s), 1577(s).

Dibenzylcarbodiimide. Polystyrene diphenylphosphine [15] 13.23 g (25% excess) was dissolved in 125 ml CH_2Cl_2. The system was cooled to 0°C, and bromide (1.31 ml, 25 mmol, 25% excess in 15 ml CH_2Cl_2) was added over a period of 30 min. The resulting suspension was stirred for an additional 10 min, and triethylamine 7.42 ml, 5.4 g, 26% excess was added. Similarly, 5 g of dibenzylurea (20.8 mmol) was added in five equivalent portions to the 0°C suspension over the next hour. 12 h after the last addition of the urea, the resultant solution was filtered to remove the catalyst. Water (100 ml) was added to the filtrate and the organic and aqueous phases were separated using a separatory funnel. After drying over sodium sulfate, the dichloromethane solution was reduced to approximately 50 ml by the use of a rotary evaporator. Addition of 300 ml pentane to the viscous and dark brown oil served to precipitate impurities such as unreacted urea. After filtration, the filtrate was distilled under reduced pressure to obtain dibenzylcarbodiimide. Yield: 1.8 g (39%). ^{1}H NMR (300 MHz, $CDCl_3$): δ (ppm) 4.3 (s, 4H, CH_2), 7.3 (d, 10H, Ar), IR (neat): 3030(m), 3015(m), 2915(m), 2820(vs), 2119(vs) cm^{-1}.

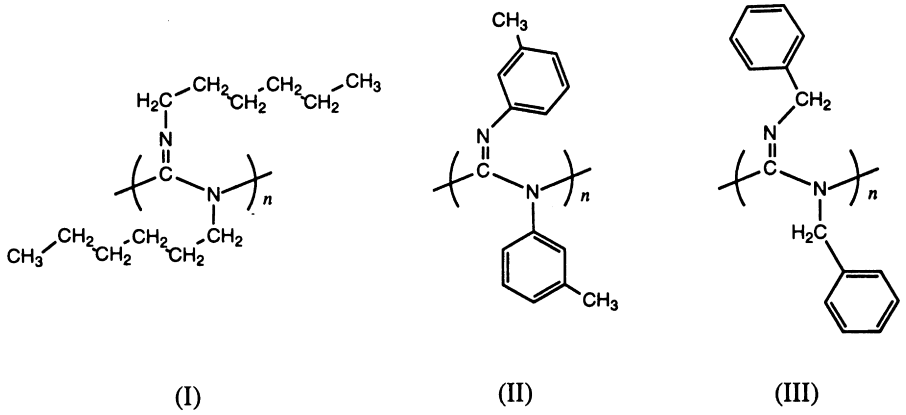

(I) (II) (III)

Fig. 1. Chemical structures of the three different polyguanidines (I), (II) and (III).

2.2. Preparation of polymers

In a dry box under Ar atmosphere, a reaction vessel was charged with a magnetic stir bar, di-*n*-hexylcarbodiimide (111.1 mg, 528 μmol), and bischloro-η^5-cyclopentadieny dimethylamido titanium(IV) (9.6 mg, 42.1 μmol). The vessel was removed from the dry box, sealed under vacuum and placed over a magnetic stir plate at room temperature. After 3 days the polymerization was quenched by the addition of wet toluene and resulting polymer purified by precipitation from methanol and lyophilization from benzene.

Similarly, poly(*N*,*N*′-di-*m*-tolylcarbodiimide), and poly-(*N*,*N*′-di-benzylcarbodiimide) were prepared by polymerization of di-*m*-tolylcarbodiimide (5.0 g, 22.5 mmol), and di-benzylcarbodiimide (3.2 g, 14.4 mmol), with bischloro-η^5-cyclopentadieny-dimethylamido titanium(IV), respectively, and purified using the same method as described above.

2.3. Solid state NMR spectroscopy

Solid state NMR experiments were performed using a Varian 300 NMR spectrometer. Cross-polarization, magic angle spinning (CP-MAS) ^{13}C NMR experiments were performed at Larmor frequency of 75.46 MHz. The samples were placed in the 7 mm CP-MAS probe as powders. The magic angle spinning rate was set at 4–6 kHz, to minimize spinning sideband overlap. The π/2 pulse time was 5 μs, corresponding to a spin-locking field strength of 50 kHz. ^{13}C $T_{1\rho}$ measurement was made by applying a ^{13}C spin-locking pulse after a 0.8 ms CP preparation period. The decay of the ^{13}C magnetization in the spin-locking field was followed for spin-locking times of up to 30 ms.

3. Results and discussion

The polyguanidines prepared for this study differed from one another in their side chains. The chemical structures of I, II, and III are shown in Fig. 1. Structural analysis of the polyguanidines were carried out by NMR spectroscopy. Fig. 2(a)–(c) shows the solid state ^{13}C CP/MAS NMR spectrum of polyguanidines (I), (II), and (III) at room temperature, respectively. The ^{13}C CP/MAS NMR spectrum of the polyguanidine (I) consisted of six signals at chemical shifts of $\delta = 149.06$, 49.36, 33.04, 28.64, 23.72, and 14.91 ppm at room temperature. The six peaks of polyguanidine (I) are assigned in Fig. 2(a). The main chain carbon of 149 ppm resonance peak has a very small relative intensity. It broadens greatly with respect to increasing temperature. The ^{13}C CP/MAS NMR spectrum of the polyguanidine (II) consisted of five signals at chemical shifts of $\delta = 148.10$, 138.26, 128.17, 119.04 and 22.09 ppm at room temperature. But, the signals of 138.26, 128.17 and 119.04 ppm are for the aromatic ring. The peaks of polyguanidine (II) are also assigned in Fig. 2(b). The ^{13}C NMR spectrum of the polyguanidine (III) show five signals at chemical shifts of $\delta =$ 149.78, 141.95, 138.59, 128.56, and 52.57 ppm. Also, the signals of 141.95, 138.59, and 128.56 ppm are for the aromatic ring, and the peaks are assigned in Fig. 2(c). The most intense signal comes from the carbons in the aromatic ring, and the main-chain carbon peak has a relatively small intensity for three samples. The spinning sidebands are marked with an asterisk. The chemical shifts for all polyguanidines (I), (II), and (III) were measured at various temperatures, and were found to be nearly independent of this variable.

The spin–lattice relaxation times in rotating frame, $T_{1\rho}$, for each carbon of the polyguanidines were taken at several temperatures with variable spin-locks on the carbon channel following cross-polarization. The ^{13}C magnetization was generated by cross polarization after a spin-locking of the protons. Then the proton rf field was turned off for a variable time *t* while the ^{13}C rf field remained on. Finally, under high power proton decoupling, the ^{13}C free induction decay was observed and subsequently Fourier transformed. Values of $T_{1\rho}$ may be obtained selectively by Fourier transformation of the FID following the end of spin-locking and repetition of the experiment with variation of time *t*. All the traces obtained in the three polyguanidines are fitted by the following

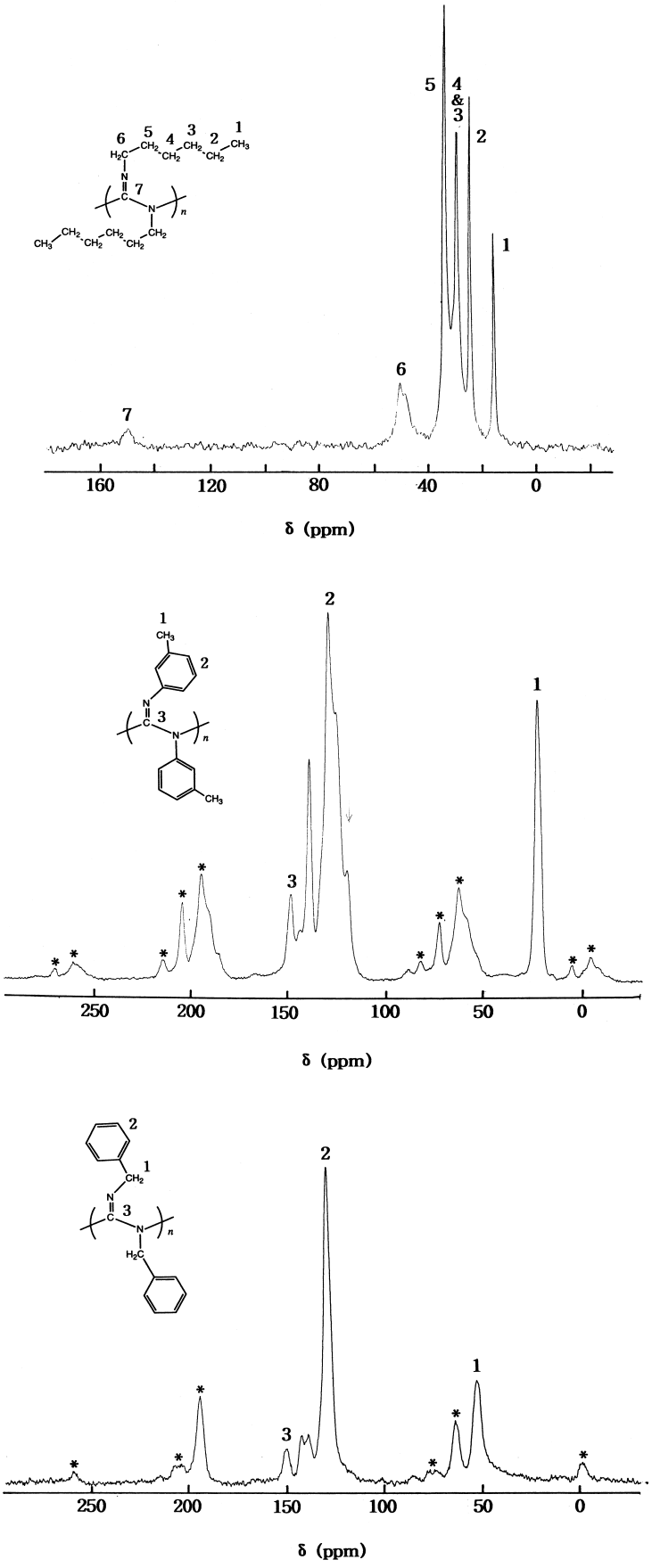

Fig. 2. Solid state ^{13}C CP/MAS NMR spectrum of polyguanidines (I), (II), and (III) at room temperature.

single exponential function [16,17]:

$$M_z(t) = M_0 \exp(-t/T_{1\rho}) \quad (1)$$

where M_z and M_0 represent the loss of the magnetization and the total nuclear magnetization of ^{13}C in thermal equilibrium, respectively.

The $T_{1\rho}$ curve has a minimum in its relaxation time vs temperature plot. For the studies of molecular motion from the experimental relaxation time, it is important to note whether the relaxation time is located on the slow side or the fast side of the minimum. This is because the slow side of the curve can be interpreted in such a way that a decrease in the $T_{1\rho}$ value indicates increased molecular motion, while the fast side of the curve can be interpreted in such way that an increase in $T_{1\rho}$ value indicates increased molecular motion [18].

The $T_{1\rho}$ for each carbon was measured as a function of temperature in polyguanidines (I), (II), and (III), respectively. In the case of the polyguanidine (I), values of ^{13}C $T_{1\rho}$ are presented in Fig. 3(a) as a function of the inverse of the temperature. The spin–lattice relaxation time of the main-chain carbon decreases with increasing temperature. This relaxation time undergoes motion on the slow side of the $T_{1\rho}$ minimum. Except for the main-chain carbon, as the temperature is increased, the ^{13}C $T_{1\rho}$ relaxation times slowly decrease, and then begin to increase passing through a minimum at 40°C. The ^{13}C $T_{1\rho}$ relaxation times of each carbon show a similar trend, and the $T_{1\rho}$ minimum in these curve occurs at 40°C. The $T_{1\rho}$ values at the minimum are 1.05, 6.49, 5.08, 14.80 and 19.86 ms for the 49, 33, 29, 24 and 15 ppm, respectively. For the 15 ppm, the $T_{1\rho}$ values are higher than that of the $T_{1\rho}$ values of 49 ppm. It is especially worth noting that the long relaxation time of 15 ppm is different from those of other carbons of the side chain. This is inconsistent with the fact that the dipolar relaxation is more efficient where the number of bounded protons is greater. The $T_{1\rho}$ values of carbons outside the side-chain show gradually increasing values. This suggests that the side chains have additional mobility due to internal rotation [19]. In general, such an increase in the $T_{1\rho}$ values of carbons has been observed in alkyl chains attached to a main polymer chain [20,21]. This increase is due to the greater mobility of the side chain toward its free end.

The $T_{1\rho}$ values for all carbons as a function of temperature in polyguanidines (II) and (III) are shown in Fig. 3(b) and (c), respectively. The spin–lattice relaxation time gradually decreases with increasing temperature. The degree of the change for all the carbons with respect to the temperature is similar, and the $T_{1\rho}$, corresponding to two peaks except in the main-chain carbon in polyguanidine (II) and (III) has a shorter relaxation time. The spin–lattice relaxation times of the main-chain carbons drastically decrease with increasing temperature as shown in Fig. 3(b). The ^{13}C $T_{1\rho}$ of the main chain in polyguanidine (II) has a longer relaxation time than polyguanidine (III), and it changes more drastically in the case of the polyguanidine (II). The $T_{1\rho}$ of the main-chain carbon is 3–8 times longer than the carbon for the aromatic ring at room temperature, due to the fact that dipolar relaxation is more efficient when a carbon has bound protons [22–24]. The relaxation times of the two polyguanidines (II) and (III) are on the slow side of the $T_{1\rho}$ minimum, and all of these carbons were determined to undergo slow motions on the low-frequency side of the $T_{1\rho}$ minimum, under slow motion conditions $\omega\tau_c \gg \omega_1\tau_c \gg 1$ [16,25]. On the slow side of the $T_{1\rho}$ minimum, a decrease in $T_{1\rho}$ results in smaller values of τ_c. Therefore, the decrease in $T_{1\rho}$ with temperature represents an increase in mobility at higher temperatures for these carbons [25].

The $T_{1\rho}$ values can be related to corresponding values of the rotational correlation time, τ_c [16]. The rotational correlation time is the length of time that a molecule remains in a given state before the molecule reorients. As such, τ_c, is a direct measure of the rate of motion. For the spin–lattice relaxation time in the rotating frame, the experimental value of $T_{1\rho}$ can be expressed in terms of a correlation time τ_c for the molecular motions by the following function [22–24].

$$T_{1\rho}^{-1} = (N/40)(\gamma_C\gamma_H\hbar/r^3)^2[4J(\omega_1) + J(\omega_H - \omega_C) + 3J(\omega_C) + 6J(\omega_H + \omega_C) + 6J(\omega_H)] \quad (2)$$

where

$$J(\omega_1) = \tau_c/[1 + \omega_1^2\tau_c^2]$$

$$J(\omega_H - \omega_C) = \tau_c/[1 + (\omega_H - \omega_C)^2\tau_c^2]$$

$$J(\omega_C) = \tau_c/[1 + \omega_C^2\tau_c^2]$$

$$J(\omega_H + \omega_C) = \tau_c/[1 + (\omega_H + \omega_C)^2\tau_c^2]$$

$$J(\omega_H) = \tau_c/[1 + \omega_H^2\tau_c^2]$$

where $J(\omega)$ is the spectrum density function, γ_C and γ_H are the gyromagnetic ratios for the ^{13}C and ^{1}H nuclei, respectively, N is the number of directly bounded protons, r is the C–H internuclear distance, $\hbar = h/2\pi$ where h is Planck's constant, ω_C and ω_H are the Larmor frequencies of ^{13}C and ^{1}H, respectively, and ω_1 is the spin-lock field. The Mathematica package was used to simulate the variations of $T_{1\rho}$ with temperature. Since all of these experiments were obtained using the spin-locking field strength ($\omega_1 = 50 \times 2\pi \times 10^3$ rad/s), each of the minima occurs when the polymer chains have τ_c ($\tau_c = 3.18$ μs); at the minimum, the correlation time τ_c of the motion causing the minimum can be inferred from $\omega_1\tau_c = 1$. The $T_{1\rho}$ minimum given by Eq. (2) is 48.7 μs, and is inconsistent with the observed minimum for each carbon at 40°C. The depth of the minimum is determined by the magnitude of the second moment, modulated by the variation of the C–H dipolar interaction [25,26]. In the case of polyguanidine (I), we carefully controlled the minima in $T_{1\rho}$ temperature

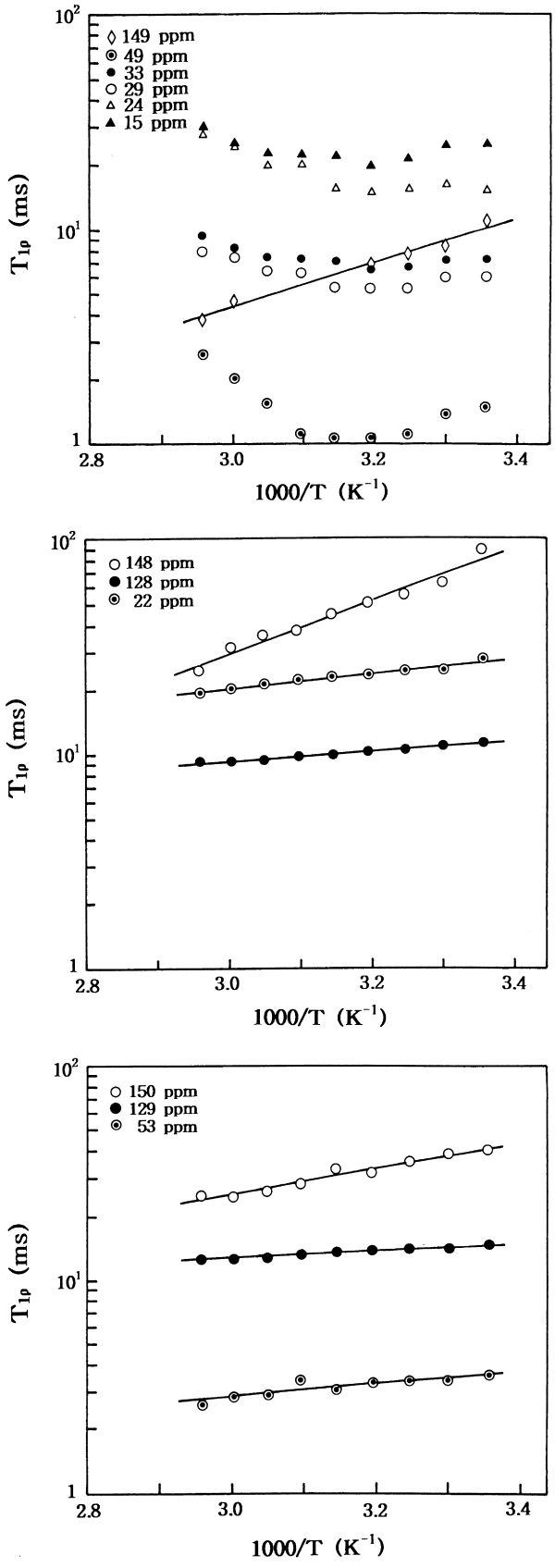

Fig. 3. Temperature dependence of ^{13}C spin–lattice relaxation time in the rotating frame, $T_{1\rho}$, for polyguanidines (I), (II), and (III).

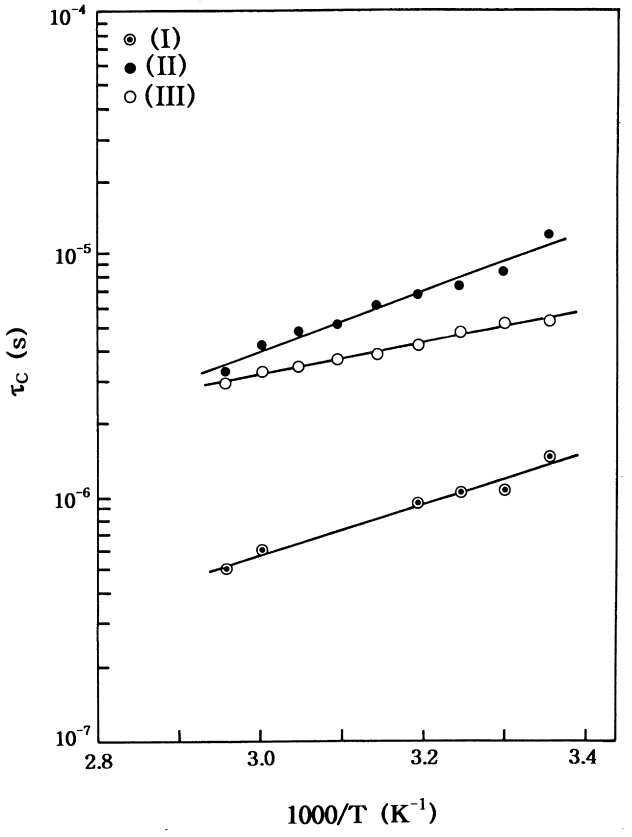

Fig. 4. Arrhenius plot of the common logarithm of the correlation times for main-chain carbons as a function of the inverse temperature for polyguanidines (I), (II), and (III).

variations and the slopes around these minima. The temperature dependence shown in Fig. 3 can be obtained by assuming an Arrhenius behavior for the motion [27]:

$$\tau_R = \tau_R^0 \exp(E_A/RT) \quad (3)$$

with T the temperature, R = 8.31 J/molK the gas constant, E_A the activation energy, and τ_R^0 the correlation time for $T \rightarrow \infty$ [28]. Thus, a plot of the natural logarithm of the correlation time as a function of the inverse temperature is linear with a slope that is proportional to the activation energy for motion. The temperature dependencies of the τ_c calculated from the relaxation time of the main-chain carbons in three polyguanidines are shown in Fig. 4. The slopes of the correlation time of (I) and (II) with increasing temperature were more drastically decreased than that of (III). The activation energies for these carbons, determined via fits of Eq. (3), are listed in Table 1. The $T_{1\rho}$ values for the main-chain carbon in three polyguanidines lie on the slow side of the $T_{1\rho}$ minimum, and have activation energies of 19.76, 23.12 and 12.64 kJ/mol, respectively. The activation energies of the main carbon of polyguanidine (I) and (II) are larger than those measured for polyguanidine (III). From these results, we determine that the motion of the main chains for polyguanidine (I) and (II) are more rigid. Also,

Table 1
Activation energies E_A obtained from Arrhenius plots of the correlation time as a function of the reciprocal temperature

(I)		(II)		(III)	
δ (ppm)	E_A (kJ/mol)	δ	E_A (kJ/mol)	δ	E_A (kJ/mol)
149	19.76	148	23.12	150	12.64
49	51.68	128	4.61	129	4.00
33	31.60	22	6.46	53	5.98
29	37.01				
24	37.81				
15	38.30				

the activation energy of the main-chain carbons for polyguanidine (II) is higher than that obtained for polyguanidine (III). The aromatic, methyl, and methylene carbons in the polyguanidine (II) and (III) have much lower activation energies, which indicates a low degree of rigidity for these carbons.

4. Discussion

The ^{13}C CP/MAS NMR results presented here indicate the mobility of the main chains of the polyguanidines vary as a function of the side chains. Each of the three polyguanidines was studied using ^{13}C CP/MAS NMR. The chemical shifts in all cases were consistent with the structures shown in Fig. 2. In all the polyguanidines, the $T_{1\rho}$ relaxations arising from the non H-bearing carbons are slower than those of the H-bearing carbons. This difference is due to the dependence of the relaxation on the inverse sixth power of the internuclear separation. The H-bearing carbons possess short C–H bond lengths (R_{C-H} in Eq. (2)), and therefore exhibit an efficient or fast relaxation. For non H-bearing carbons, the dipolar relaxation mechanism is less efficient because the internuclear distances to other nuclei are larger.

The ^{13}C spin–lattice relaxation times, $T_{1\rho}$, in the rotating frame showed increased mobility at higher temperatures. The spin–lattice relaxation times of backbone carbon for all the polyguanidines undergo slow motions, i.e. motions on the slow side of the $T_{1\rho}$ minimum. Therefore, the decrease in $T_{1\rho}$ represents an increase in mobility at higher temperatures.

The activation energy is a quantitative measure of rigidity, and can be obtained for each carbon based on the correlation times as a function of temperature. The backbone of polyguanidine (II) with aromatic side chains has a higher activation energy, 23.12 kJ/mol, than the analogous polymers with a methylene spacer between the backbone (i.e. III), 12.64 kJ/mol. The activation energies of main-chain carbons are strongly dependent on the substituent size. It is also worth noting that the activation energies of the main-chain carbon for polyguanidine (II) with the aromatic ring and methyl carbon are distinctly different from those for polyguanidine (III) aromatic ring and methylene carbon. In this case, the activation energy for polyguanidine (II) is nearly twice larger. These results show that the activation energy of backbone carbon is different due to the position of aromatic ring, and methyl or methylene carbon.

5. Conclusions

The solid-state dynamic of a series of polyguanidines using different side-chains has been measured using ^{13}C CP/MAS NMR techniques. The ^{13}C $T_{1\rho}$ spin–lattice relaxation times were measured, and from those measurements, the rotational correlation times were calculated. Finally, activation energies were obtained for the various carbons. The main-chain carbons of polyguanidines (I) and (II) have a higher activation energy than the other polyguanidine (III), indicating that the backbone dynamics is influenced by the size of the side chains.

Acknowledgements

One of the authors (A.R.L.) was supported by the Korea Science and Engineering Foundation through the Research Center for Dielectric and Advanced Matter Physics (RCDAMP) at Pusan National University (1997-2000). B.M.N. would like to acknowledge the Office of Naval Research, and the FAA for financial support.

References

[1] Shibayama K, Scott W, Seidel SW, Novak BM. Macromolecules 1997;30:3159.
[2] Goodwin A, Novak BM. Macromolecules 1994;27:5520.
[3] Schlitzer DS, Novak BM. J Am Chem Soc 1998;120:2196.
[4] Gisser DJ, Glowinkowski S, Ediger MD. Macromolecules 1991;24:4270.
[5] Ravindranathan S, Sathyanarayana DN. Macromolecules 1995;28:2396.
[6] Schaefer J, Stejskal EO, Buchdahl R. Macromolecules 1977;10:384.
[7] Lim AR, Stewart JR, Novak BM. Solid State Commun 1998;110:23.
[8] Lim AR, Schueneman GT, Novak BM. Solid State Commun 1998;109:465.
[9] Steger TR, Schaefer J, Stejskal EO, Mckay RA. Macromolecules 1980;13:1127.
[10] Schaefer J, Mckay RA, Stejskal EO, Dixon WT. J Magn Reson 1983;52:123.
[11] Palomo C, Mestres R. Synthesis 1981:373.
[12] Pattern TE, PhD thesis, University of California, Berkeley, 1984.
[13] Goodwin AA. PhD thesis, University of California, Berkeley, 1996.
[14] Smith CP, Temme GH. J Org Chem 1983;48:4681.
[15] Relles HM, Schluenz RW. J Am Chem Soc 1974;96:6469.
[16] Laupretre L, Monnerie L, Virlet J. Macromolecules 1984;17:1397.
[17] Spyros A, Dais D, Marchessault RH. J Polym Sci, Polym Phys Ed 1995;33:367.
[18] Guo M. Macromolecules 1997;30:1234.
[19] Ravindranathan S, Sathyanarayana DN. Macromolecules 1976;29:3525.
[20] Levy GC, Axelson DE, Schwartz R, Hochmann J. J Am Chem Soc 1978;100:410.
[21] Ghesquiere D, Chachaty C, Tsutsumi A. Macromolecules 1979;12:775.

[22] Bloch F. Phys Rev 1946;70:406.
[23] Bloembergen N, Purcell EM, Pound RV. Phys Rev 1948;73:679.
[24] Jones GP. Phys Rev 1966;148:332.
[25] Garroway AN, Van Der Hart DL, Earl WL. Philos Trans R Soc London 1981;A299:609.
[26] Van Der Hart DL, Garroway AN. J Chem Phys 1979;71:2773.
[27] Mcbrierty VJ, Packer KJ. Nuclear magnetic resonance in solid polymers, Cambridge: Cambridge University Press, 1993.
[28] Koenig JL. Spectroscopy of polymers, ACS professional reference book, Washington, DC: ACS, 1992.